EARTH SURFACE PROCESSES AND LANDFORMS
Earth Surf. Process. Landforms **37**, 37–51 (2012)

Published online 6 July 2011 in Wiley Online Library
(wileyonlinelibrary.com) DOI: 10.1002/esp.2187

State of Science

Fluvial and slope-wash erosion of soil-mantled landscapes: detachment- or transport-limited?

Jon D. Pelletier*
Department of Geosciences, University of Arizona, 1040 East Fourth Street, Tucson, Arizona 85721-0077, USA

Received 8 May 2010; Revised 23 May 2011; Accepted 23 May 2011

*Correspondence to: J. D. Pelletier, Department of Geosciences, University of Arizona, 1040 East Fourth Street, Tucson, Arizona 85721–0077, USA. E-mail: jdpellet@email.arizona.edu

ESPL
Earth Surface Processes and Landforms

ABSTRACT: Many numerical landform evolution models assume that soil erosion by flowing water is either purely detachment-limited (i.e. erosion rate is related to the shear stress, power, or velocity of the flow) or purely transport-limited (i.e. erosion/deposition rate is related to the divergence of shear stress, power, or velocity). This paper reviews available data on the relative importance of detachment-limited versus transport-limited erosion by flowing water on soil-mantled hillslopes and low-order valleys. Field measurements indicate that fluvial and slope-wash modification of soil-mantled landscapes is best represented by a combination of transport-limited and detachment-limited conditions with the relative importance of each approximately equal to the ratio of sand and rock fragments to silt and clay in the eroding soil. Available data also indicate that detachment/entrainment thresholds are highly variable in space and time in many landscapes, with local threshold values dependent on vegetation cover, rock-fragment armoring, surface roughness, soil texture and cohesion. This heterogeneity is significant for determining the form of the fluvial/slope-wash erosion or transport law because spatial and/or temporal variations in detachment/entrainment thresholds can effectively increase the nonlinearity of the relationship between sediment transport and stream power. Results from landform evolution modeling also suggest that, aside from the presence of distributary channel networks and autogenic cut-and-fill cycles in non-steady-state transport-limited landscapes, it is difficult to infer the relative importance of transport-limited versus detachment-limited conditions using topography alone. Copyright © 2011 John Wiley & Sons, Ltd.

KEYWORDS: soil erosion; transport-limited; detachment-limited; numerical modeling

Introduction

Transport-limited hillslopes are traditionally defined as those that are soil-covered, while detachment-limited hillslopes are those that are not soil-covered. In the landform-evolution modeling literature, however, transported-limited and detachment-limited conditions have taken on an additional meaning in the past 20 years. In the numerical modeling literature, transport-limited conditions may also refer to conditions in which erosion and deposition by flowing water is related to the gradient in sediment flux along a 1D profile (or, in 2D, as the divergence of sediment flux). Sediment flux, in turn, is related to the shear stress, power, or velocity of the flow. Early landscape evolution models of soil-covered landscapes generally assumed this type of transport-limited condition (Smith and Bretherton, 1972; Willgoose *et al.*, 1991; Tarboton *et al.*, 1992). Howard (1994a, 1994b), however, argued that the fluvial/slope-wash erosion of most hillslopes and low-order valleys is unrelated to the gradient of sediment flux. Instead, he argued, slope-wash/fluvial erosion is directly related to the shear stress, power, or velocity of the flow. Howard (1994a, 1994b) thus proposed that most soil-mantled landscapes evolve under detachment-limited conditions broadly similar to those of bedrock hillslopes, i.e. particles, once detached, are conveyed out of the area where detachment-limited conditions apply without the possibility of deposition even on shallow slopes. Since Howard (1994a, 1994b), many landform evolution models of hillslopes and low-order valleys have assumed either purely transport-limited (TL) or purely detachment-limited (DL) conditions. For example, the models of Tucker and Bras (1998), Istanbulluoglu *et al.* (2003), and Simpson and Schlunegger (2003) treat soil erosion by slope-wash/fluvial processes as purely transport-limited, while those of Moglen and Bras (1995a, 1995b) and Perron *et al.* (2008, 2009) treat soil erosion by slope-wash/fluvial processes as purely detachment-limited. The geomorphic literature has not been clear on when/where each of these conditions applies. The goal of this paper is to provide greater clarification on this issue using available data sets and theoretical models.

Following Howard (1994a, 1994b), detachment-limited (DL) landscape evolution models assume that the rate of fluvial/slope-wash erosion of soil is directly related to the shear stress,

power, or velocity of overland, rill, and/or channel flow. One example of a detachment-limited model is the stream-power model of Howard and Kerby (1983) and Seidl *et al.* (1994). In this model, erosion is proportional to a power function of drainage area and along-channel slope, minus a detachment threshold, i.e.

$$\begin{aligned}\frac{\partial z}{\partial t} &= \frac{\rho_r}{\rho_s} U - K(A^{m_d} S^{n_d} - \theta_{cd}) \quad \text{if} \quad A^{m_d} S^{n_d} > \theta_{cd} \\ &= \frac{\rho_r}{\rho_s} U \quad \text{if} \quad A^{m_d} S^{n_d} \le \theta_{cd} \end{aligned} \tag{1}$$

where z is elevation, t is time, ρ_r is the rock density, ρ_s is the soil density, U is the rock uplift rate, K is an erodibility coefficient dependent on climate and substrate erodibility, A is the contributing area, S is the along-channel slope, m_d and n_d are dimensionless coefficients, and θ_{cd} is the detachment threshold below which no erosion takes place (Howard, 1994b). In order for Equation (1) or any other DL model to apply to a soil-mantled landscape, soil, once detached, must be transported out of the domain in which DL conditions apply without the possibility of deposition. This condition may occur when the threshold for detachment is much larger than the threshold for entrainment. In such cases particles, once detached, will not settle out of the flow even on gentle slopes. Erosion on soil-mantled slopes occurs by a combination of colluvial processes (e.g. creep and bioturbation), erosion by overland flow (i.e. slope-wash erosion), rill erosion, and erosion by concentrated flow in channels (i.e. fluvial erosion). Colluvial erosion/deposition has been neglected in (1) (to focus the discussion on fluvial and slope-wash erosion rates) but it will be incorporated into the model later in the paper.

Transport-limited landscape-evolution models differ from detachment-limited models in that they relate erosion rate to the divergence of a sediment flux that depends on the shear stress, power, or velocity of overland, rill, and/or channel flow, i.e.

$$\frac{\partial z}{\partial t} = \frac{\rho_r}{\rho_s} U - \nabla \cdot \mathbf{q_s} \tag{2}$$

where $\mathbf{q_s}$ is the volumetric unit sediment flux (i.e. units of length^2/time). Many equations for sediment flux are available and no one equation is applicable in all cases. One commonly used equation computes sediment flux as a power function of drainage area and slope, minus an entrainment threshold, i.e.

$$\begin{aligned}\mathbf{q}_s &= -\kappa(A^{m_t} S^{n_t} - \theta_{ct})\hat{s} \quad \text{if} \quad A^{m_t} S^{n_t} > \theta_{ct} \\ &= 0 \quad \text{if} \quad A^{m_t} S^{n_t} \le \theta_{ct} \end{aligned} \tag{3}$$

where κ is a transport coefficient dependent on climate, grain size, and substrate erodibility, m_t and n_t are dimensionless coefficients, θ_{ct} is an entrainment threshold below which no transport takes place, and $\hat{s}$ is the unit vector in the direction of the slope aspect. In contrast to the DL model, both erosion and deposition are allowed in the TL model. Whether erosion or deposition occurs depends on the sign of the divergence of the unit sediment flux.

In motivating the case that most hillslopes evolve under DL conditions, Howard (1994b) argued that TL conditions apply only if the actual sediment flux equals the potential sediment flux, i.e. the sediment flux expected for a cohesionless substrate with no vegetation. Adopting this strict definition, Howard (1994b) concluded that 'erosion by overland flow and ephemeral filling on steep, vegetated slopes is nearly always detachment limited.' It is important to note, however, that while vegetation cover and soil cohesion certainly control a landscape's resistance to fluvial and slope-wash erosion, whether or not sediment, once detached, is transported close to the bed such that it can be redeposited down slope/valley on gentler slopes is a separate issue from whether the actual sediment flux equals the potential sediment flux. In this paper the phrase 'low-order valleys' is used to refer to colluvially-filled zones of convergent flow, with or without well-defined channels, located in the uppermost reaches of the drainage network (Benda *et al.*, 2005). The purpose of this paper is to evaluate available data that constrain the conditions under which DL and TL conditions apply in hillslopes and in low-order valleys of soil-covered landscapes and to compare and contrast the predictions of each type of model in non-steady-state landscapes.

While the relative rates of sediment detachment, entrainment, and transport on hillslopes are complex, dynamic, and difficult to accurately measure or quantify at many locations, the question of whether sediment is transported without the possibility of redeposition, leading to a DL model such as Equation (1), or carried close to the bed during repeated episodes of detachment/entrainment and redeposition, leading to a TL model in which Equation (2) applies, can be addressed using long-term sediment flux data. As Howard (1994a, 1994b) noted, few hillslopes and low-order valleys in nature can be considered to be transport-limited if the strict definition that the actual sediment flux must equal the potential sediment flux is applied. Differences between the actual sediment flux (quantified by Equation (3) or by a similar empirically derived expression) and potential sediment flux can be readily incorporated into Equation (3) and similar equations, however, simply by lowering the value of κ and/or by raising the value of θ_{ct} for specific applications. As such, the coefficients κ and θ_{ct} are empirical parameters that can incorporate spatial and temporal variations in erodibility due to the presence of surface crusts, vegetation, rock-fragment armoring, etc., that are present to some extent in all landscapes. Spatial and temporal variations in erodibility result in the actual sediment flux being lower than the potential sediment flux. Nonetheless, transport-limited conditions may still apply in many cases because sediment is transported close to the bed by repeated episodes of detachment/entrainment and redeposition within or between flood events and hence the rate of erosion/deposition is related to the divergence of the sediment flux. Studies that have measured the total load from hillslopes and low-order valleys (described in detail below) indicate that bed load, i.e. transport close to the bed by repeated episodes of detachment/entrainment and redeposition, is often the dominant mode of sediment transport, even in landscapes with significant soil cohesion, vegetation cover, and surface armoring. As such, determining the applicability of TL versus DL conditions is not simply a matter of determining whether soil cohesion or vegetation exist in the landscape. Instead, it is necessary to quantify the relative proportion of sediment derived from areas with different erodibilities and to determine the dominant conditions (TL versus DL) in those areas over multiple storm events of varying magnitude. For this reason, the question of whether TL or DL conditions predominate at a specific location is closely related to the magnitude of spatial and temporal variability in detachment/entrainment thresholds within a landscape. In this paper, both of these issues (i.e. the applicability of TL versus DL conditions and the role of variations in detachment/entrainment thresholds) are addressed by reviewing available field data and performing numerical model experiments of the evolution of ridge-and-valley landscapes.

As noted above, spatial and temporal variations in erodibility can be important controls on the relative importance of TL versus DL conditions. The threshold shear stress required to entrain sediment on a grass-covered landscape is sufficiently large (i.e. approximately 100 Pa, or 5 cm of overland flow on

a gradient of 20% (Prosser and Dietrich, 1995)) that fluvial and slope-wash erosion on hillslopes and low-order valleys is likely to be very rare under conditions of 100% vegetation cover. As such, it is likely that the relative importance of TL versus DL conditions in such landscapes is determined by conditions that predominate during episodic periods of vegetation loss (e.g. drought, fire, animal grazing) rather than conditions of 100% cover. Many surface-disturbing processes act to lower cohesion episodically through time, and it is those conditions that are most prevalent during time periods of unusually low cohesion, not the average or typical cohesion, that determines whether TL or DL conditions are dominant in a given landscape. Rain splash, for example, is effective at disaggregating and detaching soil particles from portions of the landscape that are not covered by leaves, stones, or other obstructions that limit rain drop impact. Experiments demonstrate that overland flow produced by rainfall events can be responsible for orders-of-magnitude more sediment transport than overland flow without rainfall (Eckern, 1950; Rose, 1960; Gabet and Dunne, 2003). Such experiments imply that rain splash greatly reduces the cohesion and aggregation of sediment before transport by overland flow. Furthermore, many soils lose a large majority of their subsurface cohesion as water content increases from dry to saturated conditions (Kemper and Rosenau, 1984). As such, it is the soil cohesion characteristic of high-magnitude precipitation events that is the cohesion value relevant for determining the relative dominance of TL versus DL conditions, not the dry or average conditions. Similar arguments can be made for other surface or soil-altering processes. In his study of the erosion of the Brule Formation of North Dakota, for example, Schumm (1956) found that the key process controlling fluvial and slope-wash erosion on hillslopes and low-order valleys was the reduction in soil cohesion during the cold-season months by mechanical freeze/thaw disturbance. Overland flow events in the early Spring were responsible for transporting some, but not all, of the newly unconsolidated material away. Schumm's findings are consistent with seasonal variations in soil cohesion measured in the field (Bullock *et al*., 1988) in addition to the observation that the highest sediment concentrations in fluvial channels are often measured before peak snowmelt in early Spring, when newly disturbed soil is available for entrainment, compared with similar discharges following peak snowmelt (Nanson, 1974). Given that disturbance processes such as rain splash and freeze/thaw cycles disturb the top several millimeters or more of a soil profile and that erosion rates on natural hillslopes are often less than 1 mm/yr, it is reasonable to conclude that the majority of the material eroded from many natural hillslopes and low-order valleys is in a state of low cohesion before fluvial and slope-wash transport. This line of reasoning suggests that factors besides vegetation cover and cohesion, such as texture, may be as important or more important in determining the relative importance of TL versus DL conditions.

TL and DL conditions are not mutually exclusive and, in fact, can be expected to occur concurrently in most landscapes. Indeed, there are now versions of several well-established landscape evolution models, including SIBERIA (Willgoose, 2005), CAESAR (Van De Wiel *et al*., 2007), and EROS (Davy and Crave, 2000; Davy and Lague, 2009), that recognize this fact and incorporate both TL and DL conditions using a grain-size-dependent framework for modeling detachment/entrainment and transport distance. Similarly, many event-based soil erosion models (Hairsine and Rose, 1992) incorporate soil texture within a framework that includes both DL and TL conditions as end members. Nevertheless, there are likely to be cases that are sufficiently dominated by TL or DL conditions that an end-member model may be applicable. In such cases, using a more sophisticated model that includes both DL and TL conditions may be less advantageous than using an end-member model for application over geologic time scales (i.e. to landscape evolution) because the added flexibility and sophistication of such models comes at the expense of additional model parameters that are difficult to constrain over geologic time scales.

In this paper the relative importance of TL and DL conditions in soil-covered landscapes is documented at the spatial scale of hillslopes and low-order valleys. The focus on the spatial scale of hillslopes and low-order valleys is significant for two reasons. First, hillslopes and low-order valleys comprise the vast majority of the total area of any landscape dominated by hillslope and fluvial processes. Second, it is well established that suspended load or wash load, i.e. transport of sediment high in the water column such that sediment redeposition is rare, is the dominant mode of sediment transport in most large rivers (Turowski *et al*., 2010). In contrast, the controlling factors and relative importance of suspended or wash load versus bed load on hillslopes and in low-order valleys are not well constrained. First, available field data that quantify the relative importance of bed load and suspended load sediment fluxes in cases where the soil texture has been documented are reviewed. This review indicates that bed load and suspended load sediment transport at the spatial scale of hillslopes and low-order valleys occurs in approximate proportion to the ratio of sand and rock fragments to silt and clay in the eroding soil. Second, available field measurements suggest that including spatial and temporal variations in the thresholds of detachment/entrainment is essential for making either TL or DL models compatible with field measurements. Taking those variations into account, constraints on the values of the parameters m_d, n_d, θ_{cd} and m_t, n_t, θ_{ct} in Equations (1–3) are derived consistent with available field measurements. Third, experiments with TL and DL models are performed in an attempt to identify topographic criteria that can be used to determine which condition is predominant in a given landscape. Finally, the conclusion that TL and DL conditions occur in approximate proportion to the ratio of sand and rock fragments to silt and clay in the eroding soil is used to map the relative importance of TL and DL conditions across the conterminous USA based on available soil texture data.

Analysis of and Interpretation of Field Measurements

Sediment flux data

A survey of the geomorphic literature yields two studies in which bed load and suspended load were measured for several years in small (less than or equal to approximately 10 ha) drainage basins where the fraction of sand and rock fragments to silt and clay in the soil of the watershed was also characterized. Scientists working at the Lucky Hills area of the Walnut Gulch Experimental Watershed south of Tucson, Arizona, have collected long-term data for sediment fluxes and they have characterized the soil texture at hundreds of locations. Lucky Hills 3 and 4 are small (3.68 and 4.53 ha, respectively) drainage basins located in a semi-arid climate with desert scrub vegetation. Lucky Hills 3 and 4 have mean gradients of 7.8 and 10.5%. The surficial (0–9 cm) soil at the Lucky Hills sites is a gravelly sandy loam with approximately 82% sand and rock fragments, 8% silt, and 10% clay (Nearing *et al*., 1999). Mechanical disturbance of surface crusts and seals by freeze/thaw and wetting/drying cycles appears to be an important, though not-well quantified, control on slope-wash/fluvial erosion at Walnut Gulch. In the Spring, for example, the surficial soil layer crumbles underfoot as a result of repeated freeze/thaw cycles during

the preceeding Winter months (Simanton and Renard, 1982). In addition to the supply of fine-grained sediment provided by freeze/thaw and wetting/drying cycles, rates of slope-wash/fluvial erosion are controlled by vegetation cover (canopy cover is 25% during the rainy season) and by rock-fragment armoring, which affects approximately two-thirds of the surface (Nearing *et al.*, 1999). Vegetation and rock-fragment armoring control the hydraulics of overland flow and the portion of the surface area exposed to rain splash.

Measurements of sediment flux in the valleys of Lucky Hills over a 5-year period indicate that most of the sediment is transported close to the bed by repeated episodes of detachment/entrainment and redeposition (Simanton *et al.*, 1993). In that study, sediment transport was measured in three ways. First, a traversing slot sampler was used to measure the total load by periodically moving across the width of the channel and conveying water and sediment into bottles for measurement of sediment concentration. Second, particles moving along the bed were collected in a weir and their volume was measured after each flow event. Third, a pump sampler was used to periodically sample the sediment moving up high in the water column. The purpose of the study was to test the hypothesis that the traversing slot sampler was capable of accurately measuring the total load, defined as the sum of the loads measured by the automatic pump sampler and the sediment trapped in the weir. These data can also be used to infer the predominance of sediment carried high in the water column versus sediment moving by repeated episodes of detachment/entrainment and redeposition along the bed over multiple large storm events and seasons. In this paper the sediment moving close to the bed and subject to repeated episodes of detachment/entrainment and redeposition is referred to as bed load and the sediment carried up high in the water column as suspended load. This use of bed load and suspended load is consistent with Simanton *et al.*'s (1993) interpretation of the mode of sediment transport sampled by weirs and automatic pump samplers, respectively. However, it is important to note that whether sediment, once detached, is transported with or without the possibility of redeposition, and hence whether predominantly TL or DL conditions apply, may not coincide precisely with the transition from bed load to suspended load (defined, for example, by a Rouse number threshold). Nevertheless, the transition between bed load and suspended load is a useful criterion for distinguishing between particles transported by repeated episodes of detachment/entrainment and redeposition versus sediment transported up high in the water column such that redeposition is rare.

Simanton *et al.* (1993) reported that 76% and 63% of the total sediment transported was transported as bed load in the Lucky Hills 3 and 4 basins of Walnut Gulch, respectively. These percentages are slightly lower than, but comparable with the percentage of sand and rock fragments in the surficial soil (82%). Bed load may have been more dominant in LH3 compared with LH4 because the channel system in LH3 is more deeply incised. As a result, bed load sediments are less prone to storage in the low-order valleys upstream of the measurement location in LH3 compared with LH4. It is because of this storage effect (which increases with basin area) that the literature review in this section is limited to small (<10 ha) drainage basins. If correct, this interpretation suggests that the ratio of bed load to suspended load at the hillslope scale in LH4 may be somewhat higher than the 63% measured at the flume, but that this ratio decreases downstream between the hillslope scale and valley scale (i.e. where the flume is located) due to valley-floor deposition of some of the bed load removed from the hillslope.

The importance of sediment redeposition within hillslopes and low-order valleys of Walnut Gulch has also been demonstrated using ^{137}Cs measurements in soil and fluvial sediments. In Ritchie and colleagues (Ritchie et al., 2005; 2009; Nearing et al., 2005), ^{137}Cs measurements were used to quantify hillslope erosion and deposition rates within the Lucky Hills (desert-scrub-dominated) and Kendall (grass-dominated) subwatersheds and to compute the net losses and gains from these two subwatersheds. The results of that study indicate that a large proportion of sediment entrained from hillslopes was redeposited downslope in basal swales without entering the valley network. Redeposition was particularly significant within the grass-dominated watershed. As a result, the net efflux of sediment from the grass-dominated watershed was nearly zero. The limited transport distance of particles entrained from hillslopes was also documented by Parsons *et al.* (2006). These authors found that sediment yield from hillslope-scale plots at Walnut Gulch decreases with increasing plot length for plots longer than 7 m but with similar slope, a result they interpreted to be partly a result of the increased probability of sediment redeposition at the bases of slopes in longer plots. It is worth noting that, aside from the presence of locally distributary channel networks in some locations in Walnut Gulch, sediment redeposition is generally not apparent in the field based on surficial characteristics. Sedimentation in many areas is sufficiently slow that vegetation is continually re-established in many swales where ^{137}Cs measurements indicate that fluvial or slope-wash deposition is active. As such, the absence of unequivocal evidence for deposition (e.g. unvegetated fans) should not be considered a sufficient condition for the applicability of a DL erosion model. It is also important to note that TL conditions do not require deposition in any case (Willgoose, 2005). The topography of a hillslope may be sufficiently convex that only erosion takes place in a TL landscape.

The study of Fredriksen (1970) provides complimentary data to that obtained at Walnut Gulch but in a more humid and higher-relief setting. Fredriksen measured bed load and suspended load in three watersheds of 13, 20, and 28 acres (5.3, 8.0, and 11.3 ha) in the H.J. Andrews Experimental Forest in Oregon over a 10-year period. These drainage basins are slightly larger in size, but comparable with the Lucky Hills subwatersheds at Walnut Gulch. Mean slopes of these landslide-dominated watersheds are between 53% and 63%, however, with local slopes exceeding 100%. Soil texture in these watersheds is 60% sand and rock fragments, 23% silt, and 17% clay based on data from Table 2 in Dyrness (1969). At the beginning of the monitoring period, one of the three watersheds was clear cut, one was patch cut, and one 'control' watershed was left unperturbed. The percentage of the total load that occurred as bed load was 36%, 50%, and 82% in the clear-cut, control, and patch-cut watersheds, respectively. The vast majority of the sediment derived from the patch-cut watershed (82% bed load), and from the sum of all three watersheds combined, was transported as bed load via fluvial and/or slope-wash reworking of a series of landslides triggered by an extreme storm during the winter season of 1964–1965. Given the episodic nature of landsliding, it is not surprising that the ratio of bed load to suspended load varied considerably between the three watersheds in Fredriksen's study. Nonetheless, the relatively high proportion of bed load to suspended load in the data, along with the increase in the relative importance of bed load following landsliding, suggests a dominant role for bed load transport at Fredricksen's sites averaged over time scales that include multiple landslides.

The studies of Simanton *et al.* (1993) and Fredriksen (1970) provide preliminary support for the hypothesis that the relative importance of bed load and suspended load transport at the scale of hillslopes and low-order valleys is approximately equal to the ratio of sand and rock fragments to silt and clay in the eroding soil. It should be emphasized that the relationship

between the relative importance of bed load and suspended load and soil texture requires more data for confirmation and is, at best, an approximate result. Nevertheless, this hypothesis has long been informally adopted in the geomorphic literature. Melton (1957), for example, invoked this hypothesis to explain the correlation he documented between valley side slope and wet soil strength, i.e. 'In an area of low S_w (wet soil strength), silt and clay predominate in the soil...debris brought into the channels by runoff from the slopes remains in suspension and is immediately transported out of the area... In an area of high S_w... coarse material accumulates as bed load.' (Melton, 1957, p. 33). More specifically, it has often been assumed that suspended load is the mode of transport for particles less than 0.062 mm in diameter (i.e. silt and clay) (Lane, 1982). Lane (1982) and others acknowledge the arbitrary nature of this proposed threshold diameter, however, recognizing that the threshold size below which sediment is transported in suspension is ultimately a function of shear velocity.

Calculations based on the Rouse number, however, corroborate a transition from suspended load to bed load with increasing grain diameter near the silt–sand boundary. Figure 1 plots the grain diameter, d_s, below which sediment moves in suspension as a function of the product of flow depth h and the sine of the slope angle S. Sediment is carried in suspension if the Rouse number, defined as the particle fall velocity divided by the product of the shear velocity and the von Karman constant, is less than approximately 1.2. To calculate the particle fall velocity, the method of Ferguson and Church (2004) is used, assuming a particle specific gravity of 2.65. The shear velocity, u_*, is equal to the product of gravity times flow depth multiplied by the sine of the slope angle, i.e. $u_* = \sqrt{ghsinS}$, where g is the acceleration due to gravity. As Figure 1 illustrates, the threshold diameter for suspension varies between < 0.062 mm (silt) and 0.25 mm (fine sand) for a range of representative values of $h\sin S$ for overland flow on hillslopes. At Walnut Gulch, hillslope gradients are approximately 10% and overland flow depths range from approximately 3 mm for median events to 6 mm for extreme events (Abrahams *et al.*, 1989). As such, values of $h\sin S$ at Walnut Gulch are in the range 0.3–0.6 mm, corresponding to a maximum grain diameter for suspension of approximately 0.15–0.19 mm, i.e. fine sand. This analysis probably overestimates the value of the threshold grain diameter for suspension on hillslopes because it assumes a uniform flow depth. In nature, overland flow depths are highly spatially variable (Abrahams *et al.*, 1991). Areas of relatively thin flow provide zones where the coarse fraction of suspended sediment can be redeposited both within and between storms and hence give rise to TL conditions. Despite the complexity posed by the spatial variability in overland flow depths, this analysis suggests that the transition from predominantly bed load to suspended load transport occurs for grain sizes in the range of coarse silt to fine sand for representative shear velocity conditions on hillslopes, with increasing values of d_s for steeper slopes and/or deeper runoff.

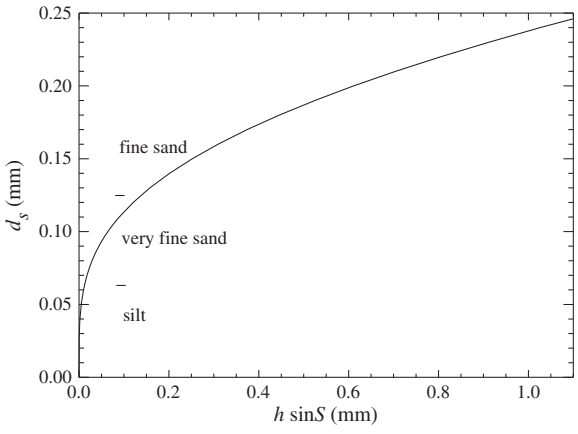

Figure 1. Illustration of the hydraulic controls on the grain size separating bed load and suspended load. Plot of the threshold grain diameter for suspended transport, d_s, versus the product of the overland flow depth h and sine of the slope angle S on hillslopes based on the Rouse number calculation described in the text. For a representative range of values of $h\sin S$, the value of d_s varies from silt to fine sand, with increasing values of d_s for deeper flow depths and/or steeper slopes.

Clearly more data are needed to conclude that the ratio of bed load to suspended load at the scale of hillslopes and low-order valleys is approximately equal to the ratio of sand and rock fragments to silt and clay. Nevertheless, the ratio of bed load to suspended load is clearly a function of sediment texture, as the analysis leading to Figure 1 illustrates, and data from the Walnut Gulch Experimental Watershed and the H.J. Andrews Experimental Forest suggests that the relative proportion of bed load to suspended load is broadly consistent with the relative proportion of sand and rock fragments to silt and clay in the eroding soil. This conclusion is also consistent with available studies of particle transport distance (Duncan *et al.*, 1987) that illustrate the persistent retention of fine sand and coarser particles and the rapid evacuation (i.e. within a time interval less than several flood events) of silt and clay particles artificially introduced to hillslopes and low-order valleys. It should again be emphasized that the association between the ratio of long-term bed load to suspended load and the ratio of sand and rock fragments to silt and clay is only approximate. As illustrated in Figure 1, very fine sand and/or fine sand can move in suspension under conditions of relatively deep runoff and/or steep gradients. In addition, silt and clay particles can be transported as bed load if transported in aggregate form.

The role of variations in erodibility on the topographic and discharge controls on sediment yield

Nearing *et al.* (1999) quantified the discharge and slope controls on sediment yield at the Lucky Hills subwatershed of Walnut Gulch described in the previous section. Using a portable sediment measuring flume and water source, Nearing *et al.* (1999) measured the sediment yield at Lucky Hills over a range of discharge conditions and documented a proportional relationship between erosion rate and the square of the product of discharge and slope, i.e.

$$E \propto (QS)^2 \tag{4}$$

where E is the erosion rate and Q is the discharge. Nearing *et al.* (1999) expressed their results in terms of unit discharge, but here total discharge is used in Equation (4) in order to facilitate comparison with Equations (1–3). Nearing *et al.* (1999) held width constant in their study, hence erosion rate is proportional to either discharge squared or unit discharge squared. The erosion rate measured by Nearing *et al.* (1999) (the total volume of all sediment, per unit time, removed from the area subject to flow) may represent either an erosion rate (as in Equation (1)) or a sediment flux (as in Equation (3)), depending on whether DL or TL conditions apply. Nearing *et al.* (1999) did not distinguish between bed load and suspended load in their study hence whether DL or TL conditions apply at the site of their experiment is unknown. Nevertheless, their data can be used to

constrain the parameters in Equations (1) or (3), depending on whether DL or TL conditions are assumed to be dominant.

The quadratic relationship between erosion rate and the product of discharge and slope documented by Nearing *et al*. (1999) is consistent with the results of a number of similar studies of fluvial and slope-wash erosion at a range of spatial scales. For example, Istanbulluoglu *et al*. (2003) inferred power-law relationships between erosion rate and drainage area (a proxy for discharge) and erosion rate and slope, with exponents of 2.1 and 2.25, respectively, using the sediment volume excavated from gullies in a study region in Idaho. A quadratic relationship between erosion rate and slope is also consistent with the results of Montgomery and Brandon (2002) at much larger spatial scales. These authors documented a power-law relationship between erosion rate (derived from suspended sediment fluxes, hence their results apply only to the DL component of fluvial and slope-wash erosion) and relief measured at a 10-km scale, with an exponent of 1.8. This nearly quadratic relationship holds for relief values between 100 and 1000 m. Above 1000 m, erosion rates increased more rapidly with slope, perhaps because mass movements supply additional sediment, unprotected by vegetation cover, that, once detached, were transported in suspension. Carson and Kirkby (1972) also provide theoretical support for Equation (4) (i.e. their equation 8.24 with $n = 3$) using an analysis that combines the Meyer–Peter–Muller bed load transport formula with overland flow governed by the Darcy–Weisbach friction formula. Nearing *et al*.'s (1999) data suggest $\theta_{cd} = 0$ and $n_d \approx 2$ or $\theta_{ct} = 0$ and $n_t \approx 2$, depending on whether sediment transport occurs as suspended load or bed load. Similarly, Montgomery and Brandon's (2002) data suggest $\theta_{cd} = 0$ and $n_d \approx 2$. The lack of a finite threshold value for detachment/entrainment in these datasets is consistent with the results of both suspended and bed load sediment yields from soil-mantled hillslopes and low-order valleys generally, i.e. suspended and bed load sediment fluxes often a power-law function of discharge (i.e. 'rating curves') with no threshold value (Milliman and Syvitski, 1992; Emmett and Wolman, 2001).

The lack of an apparent detachment/entrainment threshold in such data is, at first glance, difficult to reconcile with the basic assumption of both the DL and TL models, i.e. that sediment must be detached or entrained with a finite shear stress in order to be transported. It is clear, however, that in some portions of most landscapes there is a finite (and in some cases large) entrainment/detachment threshold, especially in areas with vegetation cover, rock fragment armoring, surface crusting, etc. As such, a finite threshold value for θ_{cd} or θ_{ct} must occur in at least some portions of nearly all landscapes. This apparent contradiction can be reconciled by the heterogeneity of most geomorphic surfaces. Nearly all landscapes have bare areas that include some component of fine sediment available for transport in minor runoff events. As such, once runoff is initiated in a storm event, sediment entrainment will occur first in relatively bare areas with the lowest resistance to erosion. As runoff increases, the shear stress induced by overland flow will be greater than the threshold value for detachment/entrainment in an increasingly large fraction of the landscape, causing an increasingly large fraction to contribute sediment to the overall yield. This conceptual model suggests that in order to relate the models of Equations (1–3) to real-world data, it is necessary to consider that the values for θ_{cd} and θ_{ct}, and perhaps κ and K, vary in both space and time at essentially all scales for most landscapes, e.g. all landcapes with significant heterogeneity in vegetation cover, surface crusting, rock fragment armoring, etc. This heterogeneity is relevant to the principal issue of this paper, i.e. determining the relative importance of TL and DL conditions, because areas of relatively high erodibility will contribute disproportionately to the total sediment yield in any landscape with variable erodibility. As such, it is the conditions (TL or DL) in areas of relatively high erodibility that play a disproportionately important role in determining whether DL or TL conditions are predominant at the landscape scale.

Spatial and/or temporal variations in sediment entrainment/detachment are also important for reconciling differing values of n_d and n_t between studies in relatively homogeneous versus relatively heterogeneous landscapes. The available sediment flux data discussed above that indicate $n_d \approx 2$ and/or $n_t \approx 2$ are at odds with several lines of evidence indicating a more nearly linear relationship between fluvial and slope-wash erosion rate and slope in areas of relatively homogeneous erodibility. The Revised Universal Soil Loss Equation (RUSLE), for example, includes a slope factor that is nearly linear with slope for gently sloping terrain with uniform erodibility (McCool *et al*., 1987). Although highly empirical, RUSLE is based on a large set of erosion rates of soil on cultivated/managed hillslopes. Field studies that have constrained the values of n_d and n_t based on erosion of relatively uniform landscapes (e.g. rapidly eroding badlands with no vegetation cover) also suggest values close to 1 (Howard and Kerby, 1983; Whipple and Tucker, 2002). Howard and Kerby (1983), for example, found that erosion rates in a badland-type DL landscape in Virginia was proportional to the 4/9ths power of drainage area and to the 2/3rds power of channel gradient. Whipple and Tucker (2002) concluded, on the basis of evidence from the published literature, that $n_t = 1$ is the most appropriate *a priori* estimate for the slope exponent in the TL model.

Introducing statistical variations into θ_{cd} and θ_{ct} into the stream-power model has the effect of making the relationship between erosion rate and stream power more nonlinear and hence such variations provide a means for reconciling empirical data indicating a nearly quadratic relationship between erosion rate and discharge/slope with no threshold value in heterogeneous landscapes with data suggesting a more nearly linear relationship between erosion rate and stream power above a threshold value in relatively homogeneous landscapes. Here this concept is illustrated with two different but complimentary analyses. In the first analysis, illustrated in Figure 2(A), a synthetic landscape was divided into 1000 subdomains and the value of θ_c (representing either θ_{cd} or θ_{ct}, depending on whether DL or TL conditions are applicable) for each subdomain was chosen from a lognormal distribution with a mean value of 1 m and a prescribed coefficient of variation C_v (i.e. the ratio of the standard deviation to the mean). The specific value chosen for this example is not critical since our goal is to illustrate how variations around the mean value affect erosion relationships at the landscape scale. The erosion rate was assumed to be a linear function of the product of discharge and slope minus a threshold value, i.e. $E \propto QS - \theta_c$ if $QS > \theta_c$, $E = 0$ otherwise. The product QS was then increased from 0.3 to 10 and the total erosion rate from the model hillslope at each value of QS was computed by calculating the value of $K(QS - \theta_c)$ for each subdomain (if $QS > \theta_c$) and summing the resulting values, assuming $\theta_c = 1$ and $K = 1$. Figure 2(A) plots the resulting relationship between E and QS for $C_v = 0$, 0.5, 1, and 2, along with plots of the expected trends if E varies linearly with QS or quadratically with QS. Introducing a finite C_v causes transport to occur in some portions of the landscape for $QS < 1$ as a result of the statistical variability in θ_c. For larger values of QS, the erosion rate follows a more nearly linear variation with QS. Taken as a whole, the relationship between E and QS is more consistent with a quadratic relationship (i.e. $E \propto (QS)^2$) than a linear relationship. The goodness of fit differs depending on the value of C_v, but a C_v of 1 yields a relationship that is very nearly quadratic, consistent with the measurements of

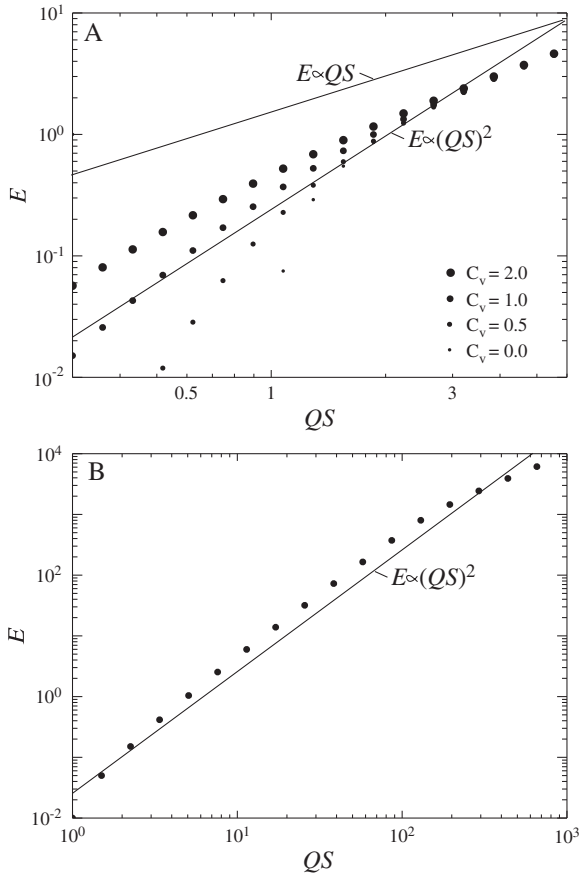

Figure 2. Illustration of the role of variability in thresholds of detachment/entrainment on the relationship between the erosion rate/sediment yield, E, and the product of discharge and slope, QS. The erosion rate locally is assumed to be a linear function of the excess stream power, i.e. $E \propto QS - \theta_c$ if $QS > \theta_c$, $E = 0$ otherwise. In (A), the total erosion rate for a hillslope with 1000 subdomains is plotted as a function of QS for a mean value of θ_c of 1 with different coefficients of variation fot θ_c. For C_v in the range 0.5 to 2.0, E increases approximately quadratically with QS. In (B), the landscape is assumed to be comprised of subdomains that have θ_c values of 1 (i.e. unvegetated) or 100 (i.e. vegetated). The model landscape is then assumed to be comprised of patches with an equal probability of taking on any vegetation cover between 0 and 100%. The plot illustrates the relationship between E and QS for 1000 simulations of the response of this model landscape to stream power values, QS, between 1 and 1000. As in (A), a nearly quadratic relationship between E and QS is predicted.

Nearing *et al*. (1999), Istanbulluoglu *et al*. (2003), and Montgomery and Brandon (2002).

Figure 2(B) illustrates the same concept using a different but complementary approach. In this analysis, the landscape is assumed to be comprised of subdomains that have θ_c values of 1 m (i.e. unvegetated) or 100 m (i.e. vegetated). The model landscape is then assumed to be comprised of patches with an equal probability of taking on any vegetation cover between 0 and 100%, i.e. patches that have no vegetation have a detachment/entrainment value of 1, those that are fully vegetated have a threshold value of 100. Those with partial vegetation cover have an intermediate threshold value given by a weighted average between 1 and 100 that depends on vegetation cover. Figure 2(B) illustrates the relationship between E and QS for 1000 simulations of the response of this model landscape to stream power values, QS, between 1 and 1000. As in the alternative analysis shown in Figure 2(A), the result is nearly quadratic. As the value of QS increases, a larger fraction of the heterogeneous landscape contributes to the total erosion rate, thereby increasing the erosion rate nonlinearly with stream power despite the fact that the erosion rate within individual subdomains has a linear relationship with QS above a (locally variable) threshold value.

The analyses in this section suggests that spatial and temporal variations in the threshold for detachment/entrainment can reconcile the apparent contradiction between theoretical models of fluvial and slope-wash erosion that include a finite detachment/entrainment threshold and empirical data that document a nonlinear relationship between erosion rate and QS with no threshold value. These results also suggest that Equations (1) and (3) are consistent with available field measurements if $n_d = n_t = 1$ are assumed and θ_{cd} and θ_{ct} are allowed to take on a range of values with $C_v \sim 1$. Alternatively, a more nonlinear relationship (i.e. $n_d \approx n_t \approx 2$) in Equations (1) and (3) with no threshold value for detachment/entrainment may be appropriate for some applications. This latter approach effectively incorporates the fact that erosion is 'activated' in more of the landscape as the stream power increases with discharge/drainage area and slope. Either approach can be adopted, since both result in predictions broadly consistent with measured sediment yields.

Numerical Modeling of Detachment-limited Versus Transport-limited Conditions

Given the difficulty of measuring the relative proportion of long-term bed load and suspended load sediment fluxes at the scale of hillslopes and low-order valleys, it is useful to ask whether there are any topographic attributes or measures that can be used to determine the relative importance of TL or DL conditions. As noted previously, there are unlikely to be any surficial characteristics, e.g. clear evidence of deposition, unperturbed by vegetation growth or bioturbation, capable of distinguishing between landscapes dominated by TL versus DL conditions. Nevertheless, there may be qualitative or quantitative signatures of TL versus DL conditions in topography that numerical modeling can identify.

Before illustrating the results of numerical models aimed at addressing this question, it is important to discuss some technical points. The numerical models of this section compute the fluvial and slope-wash erosion rate at points within the dominant fluvial pathway in each pixel, with the width of the fluvial/slope-wash pathway assumed to be equal to or smaller than the pixel width. Fluvial and slope-wash erosion is quantified using the unit contributing area (i.e. the contributing area per unit width of flow), A/w, where w is the width of flow in the dominant fluvial/slope-wash pathway within each pixel, rather than the contributing area itself. This approach is advantageous because contributing areas, as calculated using flow-routing algorithms commonly used in the geomorphic literature, are not independent of grid resolution (Schoorl *et al*., 2000). Equation (1) can be rewritten as a function of unit contributing area as

$$\frac{\partial z}{\partial t} = \frac{\rho_r}{\rho_s} U - K\left(\left(\frac{A}{w}\right)^{p_d} S^{n_d} - \theta_{cd}\right) \quad \text{if} \quad \left(\frac{A}{w}\right)^{p_d} S^{n_d} > \theta_{cd}$$

$$= \frac{\rho_r}{\rho_s} U \quad \text{if} \quad \left(\frac{A}{w}\right)^{p_d} S^{n_d} \le \theta_{cd} \qquad (5)$$

where p_d is a dimensionless coefficient. The value of w in (5) corresponds to the width of flow in the dominant fluvial/slope-wash pathway within each pixel, which may be a channel within a valley, rills or zones of concentrated overland

flow on a hillslope, or the entire pixel if flow occurs as sheetflooding.

In tributary valleys, it is often a good approximation to assume that the width of flow in the dominant fluvial/slope-wash pathway within each pixel is proportional to a power function of the contributing area (a proxy for discharge), i.e.

$$w_v = cA^b \tag{6}$$

where $b \approx 1/2$ and c is a dimensionless coefficient. The value of b is a combination of the power-law exponent relating width to discharge and the power-law exponent relating discharge to contributing area. For low-order valleys (i.e. those with contributing areas less than approximately 40 ha), Goodrich *et al.* (1997) documented a nearly linear relationship between peak discharges and contributing area at Walnut Gulch. At larger drainage areas, channels in arid regions such as Walnut Gulch increase with a smaller exponent due to channel transmission losses and declining storm area coverage. These factors are less significant in the low-order valleys focused on in this paper, hence a linear relationship between area and discharge can be assumed at these scales even in arid environments. Channel widths scale with the discharge to the 0.4–0.5 power (Leopold and Maddock, 1953), although data is sparse for low-order valleys where flow is highly episodic. Substituting Equation (6) into Equation (5) and subsuming the coefficient c into K and θ_{cd} yields (1), the familiar form of the stream-power erosion model for soil-covered landscapes (Howard, 1994b; Perron *et al.*, 2008, 2009) where $m_d = p_d - b$. If $p_d = 1$ and $b = 1/2$, for example, $m_d = 1/2$.

On hillslopes, the width of flow in each pixel is equal to the pixel width δ, i.e. $w_h = \delta$, if flow occurs as sheetflooding. Alternatively, if flow occurs in rills or microtopographically generated zones of concentrated runoff, the width of flow in each pixel is equal to $w_h = (w_r/\lambda_r)\delta$, where w_r is the width of flow in each rill/zone during high-magnitude storm events and λ_r is the mean rill/zone spacing. When applying (5) to modeling specific real-world landscapes, the value of the scaling ratio w_r/λ_r between w_h and δ must be constrained based on site-specific data for the fraction of hillslope area subject to fluvial or slope-wash erosion during high-magnitude storm events.

For simplicity, the models of this paper assume that soil continuously covers the landscape. As such, fluvial/slope-wash and colluvial erosion/deposition are included in every pixel. Colluvial transport on vegetated or partially vegetated hillslopes of low to moderate relief is often dominated by creep, rain splash, and/or bioturbation. The classic approach to modeling the evolution of hillslopes dominated by these processes is the diffusion equation (Culling, 1960, 1963):

$$\frac{\partial z}{\partial t} = D\nabla^2 z \tag{7}$$

where D is the diffusivity. In order to properly apply Equation (7) to a model in which the elevation variable z represents the elevation of dominant fluvial/slope-wash pathway within each pixel, it is necessary to scale the colluvial erosion/deposition rate (given by Equation (7)) by the ratio δ/w. This scaling is necessary because, in valleys the rate of deposition that occurs in the fluvial/slope-wash pathway within each pixel is systematically underpredicted by Equation (7) because the fluvial/slope-wash pathway is not resolved in cross-section. The cross-sectional curvature is equal to the difference in the gradients of the two side slopes adjacent to the fluvial/slope-wash pathway, divided by the width of that pathway. In a grid in which the flow width is narrower than the pixel width, the curvature will, therefore, be underestimated by a factor of δ/w, assuming that the gradients of the side slopes are adequately resolved. Applying the δ/w scaling factor to Equation (7) and combining it with Equation (5) yields

$$\begin{aligned}\frac{\partial z}{\partial t} &= \frac{\rho_r}{\rho_s}U + \frac{\delta}{w}D\nabla^2 z - K(a^{p_d}S^{n_d} - \theta_{cd}) \quad \text{if} \quad a^{p_d}S^{n_d} > \theta_{cd} \\ &= \frac{\rho_r}{\rho_s}U + \frac{\delta}{w}D\nabla^2 z \qquad\qquad \text{if} \quad a^{p_d}S^{n_d} \le \theta_{cd}\end{aligned} \tag{8}$$

for the DL model, where $a = A/w$, and, for TL model,

$$\frac{\partial z}{\partial t} = \frac{\rho_r}{\rho_s}U + \frac{\delta}{w}D\nabla^2 z - \nabla\cdot\mathbf{q_s} \tag{9}$$

where

$$\begin{aligned}\mathbf{q_s} &= -\kappa(a^{p_t}S^{n_t} - \theta_{ct})\hat{s} \ \text{ if } \quad a^{p_t}S^{n_t} > \theta_{ct} \\ &= 0 \qquad\qquad\qquad\qquad \text{if} \quad a^{p_t}S^{n_t} \le \theta_{ct}\end{aligned} \tag{10}$$

The unit contributing area is calculated in the models of this section using the D∞ algorithm of Tarboton (1997), modified to distinguish hillslopes and valleys and apply the appropriate value of w as described by Pelletier (2010). The models used here solve Equation (8) for the DL model and Equations (9) and (10) for the TL model, assuming a gently sloping (1%) initial landscape. Observed slope–area relationships in channels (e.g. $S \propto A^{-g}$ with g in the range 0.35 to 0.6) imply that p_d/n_d is in the range approximately 0.7 to 1.2 and p_t/n_t is in the range approximately 1.7 to 2.2, assuming $w_v \propto A^{1/2}$. Channel gradients are often observed to be a power-law function of drainage area with an exponent between −0.35 and −0.6 for both DL and TL conditions (Hack, 1957; Tarboton *et al.*, 1992; Ijjasz-Vasquez and Bras, 1995; Whipple and Tucker, 1999). This implies values for m/n between approximately 0.35 and 0.6 if DL conditions and steady state are assumed, i.e. $m_d =$ 0.35 to 0.6 or $p_d = 0.7$ to 1.2 if $n_d = 1$. In the previous section, it was shown that results consistent with field observations could be obtained *either* by using a linear model (i.e. $p_d = 0.7$ to 1.2 with $n_d = 1$) with a stochastic threshold *or* a nonlinear model (i.e. $p_d = 1.4$ to 2.4 with $n_d = 2$) with no threshold. In the models of this section linear models with a stochastic threshold are used because this choice was found to be more computationally efficient than assuming $n_d = 2$ or $n_t = 2$ with no threshold. For steady state to be achieved in the TL model, the unit sediment flux must be proportional to the unit contributing area, implying a value for $\frac{1}{2}(p - 1)/n$ between approximately 0.35 and 0.6 (Tarboton *et al.*, 1992; Istanbulluoglu *et al.*, 2003), i.e. $p_t = 1.7$ to 2.2 if $n_t = 1$. The fluvial/slope-wash erosion component of each model is solved at each time step of the model by calculating S in the downslope direction using a time step that satisfies the Courant stability criterion. The diffusive component of each model is calculated using an implicit numerical method that is stable for all time steps. In both cases (DL and TL models), θ_{cd} and θ_{ct} are allowed to take on a range of values characterized by a lognormal distribution with a specified mean and coefficient of variation sampled at an appropriate time interval (nominally every 100 yr).

Model results indicate that the values of the coefficient of variation of θ_{cd} and θ_{ct} exert a first-order control on the geometry of drainage networks. Figure 3 illustrates drainage basins predicted by the DL model (Equation (8)) with the same mean value for θ_{cd} but different values of the coefficient of variation, i.e. $C_v = 0$, 0.5, and 1. These results were generated from the DL model with $p_d = 2/3$, $n_d = 1$, $(\rho_r/\rho_s)U = 0.1$ m/kyr, $D = 1$ m^2/kyr,

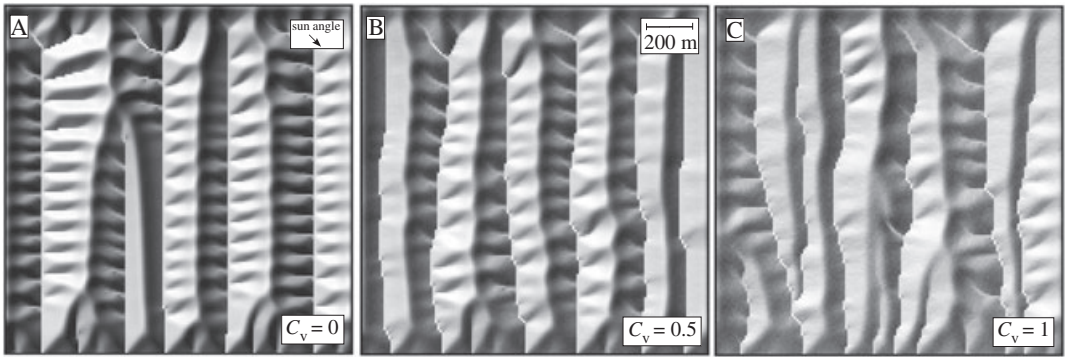

Figure 3. Illustration of the relationship between drainage basin form and the coefficient of variation of θ_c in the DL model. Shaded-relief images of topography produced by the DL model for C_v = (A) 0, (B) 0.5, and (C) 1. These results were generated from the DL model with an initial slope of 1% and $p_d = 2/3$, $n_d = 1$, $(\rho_r/\rho_s)U = 0.1$ m/kyr, $D = 1$ m^2/kyr, $K = 0.005$ m$^{1/3}$kyr^{-1}, $c = 0.01$, and $\theta_c = 10$ m$^{2/3}$ and assuming sheetflooding conditions on hillslopes (i.e. $w_h = \delta$) for a model domain 1.5 km × 1.5 km and a model duration of 10 Myr.

$K = 0.005$ m$^{1/3}$kyr^{-1}, $c = 0.01$, and $\theta_c = 10$ m$^{2/3}$ and assuming sheetflooding conditions on hillslopes (i.e. $w_h = \delta$) for a model domain 1.5 km × 1.5 km and a model duration of 10 Myr (i.e. long enough for an approximate topographic steady state condition to be achieved). In landform evolution modeling, it is common practice to use random initial topography (e.g. microtopography represented by white or colored noise) because all landscapes have some microtopography and because random initial topography is generally considered to be necessary in order to create 'realistic-looking' drainage networks if no other source of heterogeneity exists. In the model landscapes of Figure 3, however, no initial microtopography was assumed. In the case of a constant, uniform value for θ_{cd} (i.e. $C_v = 0$ illustrated in Figure 3(A)), the model produces a drainage pattern characterized by a rectangular or trellis architecture, uniformly spaced first-order valleys, and remarkably consistent tributary junction angles. As the value of C_v increases from 1 to 3 (Figure 3(B) and 3(C)), the drainage networks become more variable in planform geometry and exhibit the parallel and/or dendritic architectures characteristic of most natural drainage basins that lack structural control. These results do not prove that variability in detachment/entrainment thresholds is more important than initial microtopographic variability in controlling drainage basin form. Nevertheless, they do suggest that the variability of soil properties may be as important, or more important, a controlling factor of drainage basin form as initial microtopography. These results are not the first to document the role of variations in substrate resistance to erosion in controlling drainage basin form. Moglen and Bras (1995a, 1995b), for example, documented the dependence of drainage basin morphology on spatial variations in K in Equation (1) and concluded that some heterogeneity is required in order for model drainage basins to exhibit statistical measures (i.e. cumulative area distributions) similar to those of natural drainage basins. The results presented here are broadly compatible with those of Moglen and Bras (1995a, 1995b) but they differ in that heterogeneity is included in the detachment threshold θ_{cd}, assumed to be zero in Moglen and Bras (1995a, 1995b). This distinction is significant given the important role of variations in θ_{cd} and θ_{ct} discussed in the previous section.

In topographic steady state, landscapes produced with the DL and TL models are qualitatively similar, as landscape evolution models produced with DL and TL models over the past 20 years have illustrated. Indeed, the similarity in landscape form predicted by these two end-member model types is one reason that both types have been applied to broad geomorphic questions (e.g. controls on drainage density) despite the lack of a firm basis for applying one or the other type of model. Figures 4(A) and 5(A) illustrate landscapes driven to an approximate steady-state condition with the DL and TL models, respectively. Figure 4(A) was produced from a DL model using $p_d = 1$, $n_d = 1$, $(\rho_r/\rho_s)U = 0.1$ m/kyr, $D = 1$ m^2/kyr, $K = 0.0005$ kyr^{-1}, $c = 0.01$, θ_c with a mean value of 10 m and a C_v of 1, rilled hillslopes with $w_h = 0.1\delta$, and a model domain of 250 m × 750 m. Figure 5(A) was produced from a TL model using $p_t = 5/3$, $n_t = 1$, $(\rho_r/\rho_s)U = 0.1$ m/kyr, $D = 1$ m^2/kyr, $\kappa = 0.0001$ m$^{2/3}$/kyr, $c = 0.01$, θ_c with a mean value of 1 m and a C_v of 1 and rilled hillslopes with $w_h = 0.1\delta$, and a model domain of 250 m × 750 m. In an

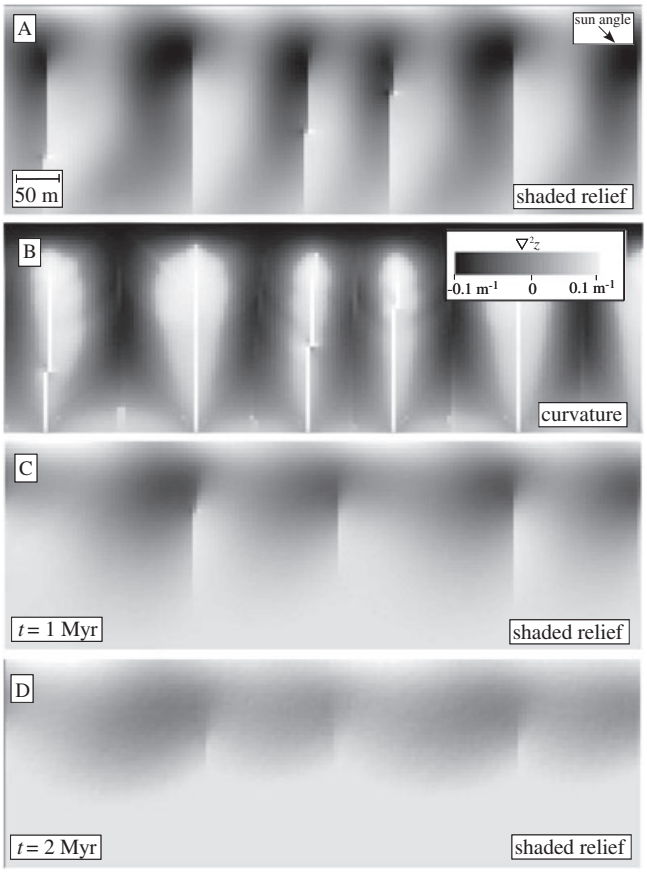

Figure 4. Evolution of a model DL landscape driven to an approximate steady state condition (shown in (A) and (B)) followed by topographic decay (i.e. uplift rate set to zero) (shown in (C) and (D)). Model parameters are $p_d = 1$, $n_d = 1$, $(\rho_r/\rho_s)U = 0.1$ m/kyr, $D = 1$ m^2/kyr, $K = 0.0005$ kyr^{-1}, $c = 0.01$, θ_c with a mean value of 10 m and a C_v of 1, rilled or concentrated flow on hillslopes with $w_h = 0.1\delta$, and a model domain of 250 m × 750 m. (A), (C) and (D) illustrate topography/elevation, (B) illustrates topographic curvature.

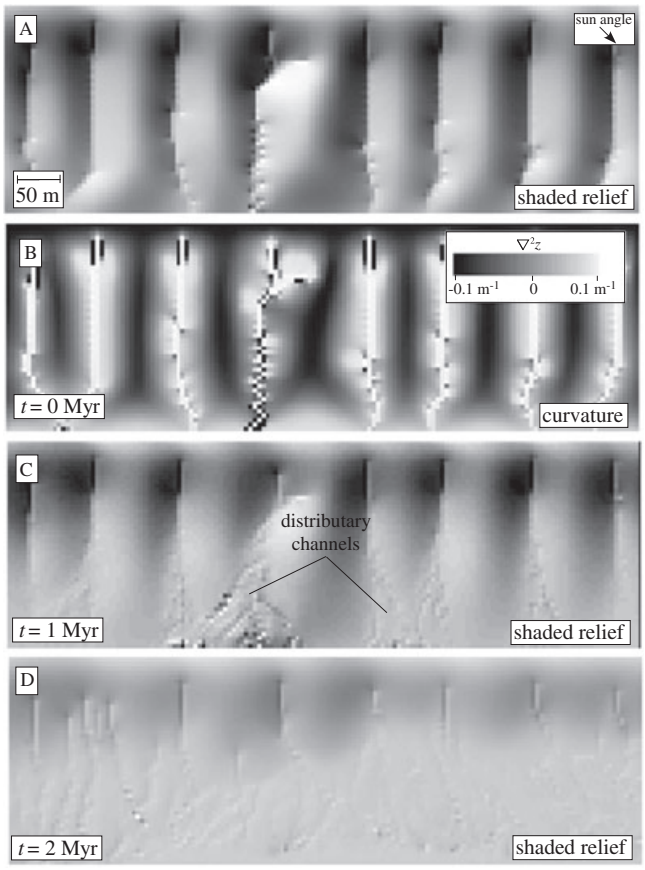

Figure 5. Evolution of a model TL landscape driven to an approximate steady state condition (shown in (A) and (B)) followed by topographic decay (i.e. uplift rate set to zero) (shown in (C) and (D)). Model parameters are $p_t = 5/3$, $n_t = 1$, $(\rho_r/\rho_s)U = 0.1$ m/kyr, $D = 1$ m^2/kyr, $\kappa = 0.0001$ m$^{2/3}$/kyr, $c = 0.01$, and θ_c with a mean value of 1 m and a C_v of 1, rilled or concentrated flow on hillslopes with $w_h = 0.1\delta$, and a model domain of 250 m × 750 m. (A), (C) and (D) illustrate topography/elevation, (B) illustrates topographic curvature.

approximate steady-state condition, hillslopes in both models have a similar morphology, i.e. they are predominantly convex near the divide and transition from convex to concave with increasing distance towards the valley head, as illustrated in the curvature maps in Figures 4(B) and 5(B).

It is useful to expand the TL model equations to identify the relative importance of advection and diffusion of topography in the DL versus the TL case. Consider, for simplicity, Equations (9) and (10) with $\theta_{ct} = 0$, $p_t = 2$ and $n_t = 1$. In that case, the TL model becomes

$$\frac{\partial z}{\partial t} = \frac{\rho_r}{\rho_s} U + \frac{\delta}{w} D \nabla^2 z + \kappa \nabla \cdot \left(a^2 \nabla z \right) \qquad (11)$$
$$= \frac{\rho_r}{\rho_s} U + \left(\frac{\delta}{w} D + \kappa a^2 \right) \nabla^2 z + \kappa \nabla \left(a^2 \right) \cdot \nabla z$$

In Equation (11), the along-channel slope S is represented by ∇z. Equation (11) illustrates that the TL model, like the DL model, combines diffusion of topography with area-dependent advection of topography. The TL model has two key differences from the DL model, however. The advection term in the TL model is equal to $\kappa \nabla (a^2) \cdot \nabla z$, while in the DL model it is equal to $K\, a |\nabla z|$, for the reference cases $\theta_{ct} = 0$, $p_t = 2$ and $n_t = 1$ and $\theta_{cd} = 0$, $p_d = 1$ and $n_d = 1$. If a scales approximately linearly with distance from the divide, i.e. if the gradient of a^2 along the valley slope is equal to a, the advection terms in the TL and DL models will have approximately the same area dependence, suggesting that any distinction between TL and DL conditions based on topography alone may be difficult to identify in steady state. However, topographic diffusion in the TL model includes an additional area-dependent diffusion term that is not present in the DL model. Nevertheless, this additional diffusion term becomes significant relative to the colluvial diffusion term only as the unit contributing area a becomes large. Portions of the landscape with relatively large a (i.e. valleys) represent only a small fraction of the total landscape and are the portions of the landscape most likely to be influenced by factors unrelated to diagnostic differences between DL and TL conditions, e.g. changes in base level. These considerations suggest the potential difficulty of distinguishing between DL- and TL-dominated landscapes based on topography alone.

Figures 4 and 5 also illustrate the DL and TL model landscapes modeled forward in time following a cessation of rock uplift. Figure 4(C) and 4(D) illustrate the topography predicted by the DL model at two time periods (i.e. $t = 1$ and 2 Myr) following the cessation of uplift, while Figure 5(C) and 5(D) illustrate the analogous result for the TL case. In the DL case (Figure 4(C) and 4(D)), topographic decay occurs as a combination of advective slope retreat and diffusive smoothing. Hillslopes in the DL model develop significant basal concavity over time as the topography decays. Concave hillslope bases are often associated with deposition, but in this case they develop despite the purely erosional nature of fluvial/slopewash processes in the model. In the TL case (Figure 5(C) and 5(D)), the slope evolution is broadly similar to that of the DL cases. Valley floors in the TL case, however, undergo autogenetic cycles of aggradation and incision not present in the DL model. In these cycles, valley-floor and sideslope deposition leads to a more distributary flow pattern that, in turn, promotes further aggradation in a positive feedback until the outlet channel fan develops a sufficiently steep slope to trigger reincision and channel narrowing in a positive feedback. During the course of the model run illustrated in Figure 5, each valley floor channel undergoes many such cycles of cutting and filling. Despite the presence of these cut-and-fill cycles and the associated distributary channel networks in valley floors of the TL model, the hillslope morphology in both cases is, at any given point in time, qualitatively similar. These results suggest that distributary channel networks and episodically incised valley floors present in non-steady-state TL-dominated landscapes are the primary qualitative differences between landscapes formed with DL versus TL conditions.

It is useful to compare the results of Figures 4 and 5 with real-world examples in which the predominance of DL versus TL conditions can be reasonably well constrained. Figure 6(A) illustrates a shaded-relief image of a LiDAR-derived bare-ground DEM of a small watershed in Walnut Gulch, a landscape dominated by TL conditions based on the results of Simanton *et al.* (1993) and the discussion earlier in the paper. Hillslopes in this drainage basin are concave at their base and exhibit a qualitatively similar form to those of both Figures 4 and 5, as illustrated by the curvature map in Figure 6(B) calculated on an 8 m scale (i.e. the 1 m/pixel was subsampled to 8 m/pixel prior to the calculation of curvature). The presence of this basal hillslope concavity is not diagnostic, however, as it is also present to a similar extent in both Figures 4(B) and 5(B). Distributary channels (Figure 6(C)), however, which are diagnostic of active deposition (Weissmann *et al.*, 2010), are present in this drainage basin. In addition, recent incision has occurred along the valley floor of this drainage basin, exposing Holocene colluvial and alluvial deposits (Osterkamp, 2008). The Holocene sediments exposed in this and other incised valleys in this watershed contrast with the much older (mid-to-late Cenozoic) Gleeson Road and Emerald Gulch

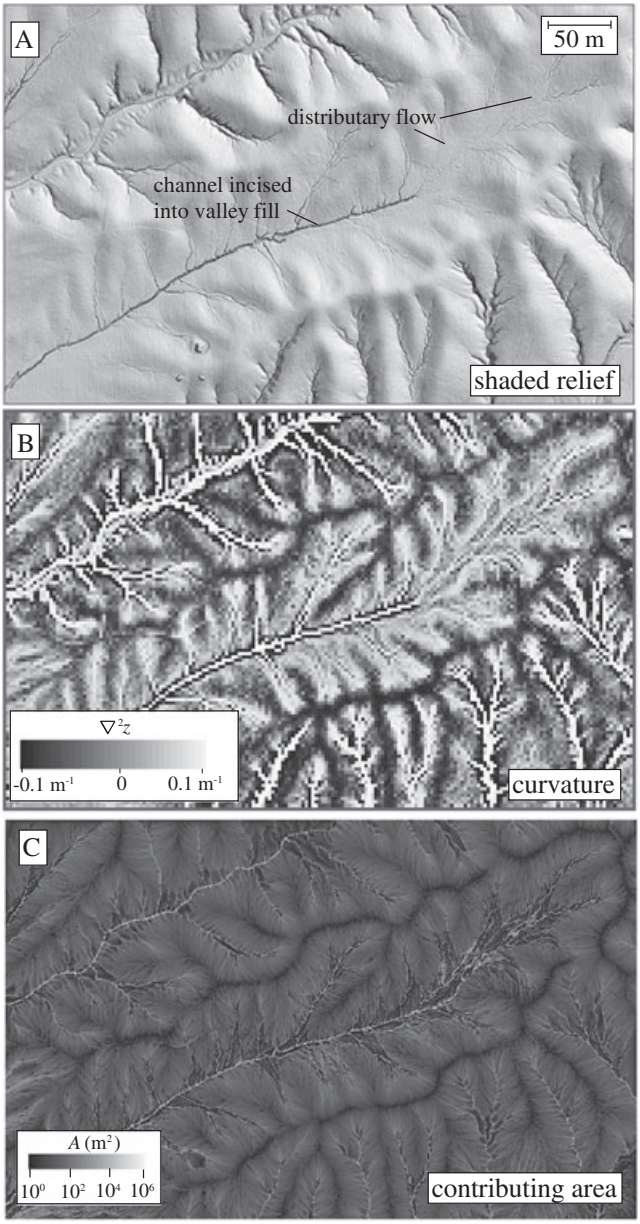

Figure 6. Example of real-world landscape illustrating diagnostic features of TL landscapes. (A) Shaded-relief image of a LiDAR-derived bare-ground DEM of a small watershed in Walnut Gulch. Hillslope bases in this drainage basin are concave and exhibit a qualitatively similar to those of both Figures 4 and 5 as illustrated by the curvature map in (B) calculated on an 8 m scale (i.e. the 1 m / pixel was subsampled to 8 m/pixel prior to the calculation of curvature). However, this basin exhibits two diagnostic features of TL landscapes in non-steady-state cases, i.e. the presence of distributary channels (best illustrated using the contributing area grid shown in (C)), and incision along the valley floor, exposing Holocene colluvial and alluvial deposits.

conglomerates that comprise the parent material on the hillslopes in this portion of Walnut Gulch (Osterkamp, 2008). Aside from the presence of distributary channels and the exposure of young sediments in the valley floor by recent channel incision, however, there do not appear to be any topographic attributes or measures uniquely consistent with DL (Figure 4) or TL (Figure 5) conditionsin this watershed.

Perron *et al*. (2009) proposed a method for distinguishing DL conditions and extracting the ratio D/K based on topography alone. Here their method is applied to the model results with DL and TL conditions to test the ability of their method to identify DL conditions. In their method, the ratio D/K is extracted from high-resolution DEMs via theoretical relations for steady-state DL landscapes. The value of D/K is then used to infer the value of a characteristic length scale L_c that relates to the spacing of first-order valleys in a systematic way. Perron *et al*. (2009) showed that landscapes produced by their numerical model, which assumes DL fluvial/slope-wash erosion of soil with $\theta_{cd} = 0$, exhibit the relation $6.4 \leq \lambda/L_c \leq 12.7$, where λ is the mean spacing of first-order valleys. Perron *et al*. (2009) concluded from their analysis that landscapes that yield $6.4 \leq \lambda/L_c \leq 12.7$ are uniquely consistent with DL conditions and $\theta_c = 0$.

Here it is shown, however, that the Perron *et al*. (2009) method does not distinguish between TL and DL conditions and yields results consistent with $6.4 \leq \lambda/L_c \leq 12.7$ for a broad class of undulating surfaces. First, consider the steady-state DL and TL models of Figures 4 and 5. The values of D/K and m for these landscapes were constrained from the intercept and slope of a least-squares linear fit to the logarithmically binned averages of S^*, defined as $|\nabla z|/(\nabla^2 z - \nabla^2 z_h)$ (where $\nabla^2 z_h$ is the average curvature as $A|\nabla z| \rightarrow 0$) and A, following the procedure outlined in Perron *et al*. (2009). L_c was then calculated using

$$L_c = \left(\frac{D}{K}\right)^{\frac{1}{2m+1}} \tag{12}$$

The ratio λ/L_c is 6.5 for the DL landscape of Figure 4(A) (i.e. the spacing of first-order valleys is 140 m and the value of L_c extracted from Equation (12) is 21.6) and 8.5 for the TL landscape of Figure 5(A) (i.e. the average spacing of first-order valleys is 95 m and the value of L_c extracted from Equation (12) is 11.2). The fact that the DL and TL models both yield results consistent with $6.4 \leq \lambda/L_c \leq 12.7$ suggests that this range of values of λ/L_c is not diagnostic of DL conditions or of vanishing θ_c.

This conclusion is further supported by the fact that the relationship $6.4 \leq \lambda/L_c \leq 12.7$ is consistent with a 'null' hypothesis consisting of a simple mathematical function that approximates the shape of valleys but has no geomorphic significance. This analysis also shows that the value of λ/L_c depends primarily on the spacing of second-order to first-order valleys rather than some aspect of the topography unique to DL conditions or a particular value of θ_c. Consider the synthetic landscape produced by the 2D sinusoidal function (Figure 7(A))

$$h = h_0 \sin\left(\frac{\pi x}{\lambda_x}\right)\left(1 - \left|\frac{x - \lambda_x/2}{\lambda_x/2}\right|\left(1 - \left|\sin\left(\frac{\pi y}{2\lambda_y}\right)\right|\right)\right) \tag{13}$$

Equation (13) contains first- and second-order 'valleys' with spacings λ_y and λ_x, respectively. Equation (13) is not a solution to any geomorphic model but is simply a mathematical function that is periodic in both dimensions and transitions from convex to concave with increasing distance from the divide. Equation (13) satisfies the relation proposed by Perron *et al*. (2009) for DL landscapes and it yields approximate power-law relationships between slope and area for a wide range of values of λ_x and λ_y. Figure 7(B) plots the values of S^* and A for a specific example with $\lambda_x = 200$ m and $\lambda_y = 25$ m. The values of D/K, m, and λ_y/L_c values in this example are 2.4 m, 0.47, and 10.4, respectively. It should be noted that the value of λ/L_c obtained from this analysis is not unique since it varies slightly with the size of the domain used to measure $\nabla^2 z_h$($A < 10\,\text{m}^2$ was used for the example in Figure 7(B)) and the range of area values used to fit S^* versus A ($A > 20\,\text{m}^2$ was used for the example in Figure 7(B)). This procedure was repeated for a total of 15 cases with a range of values of λ_x (from 200 to 800 m) and λ_y (from $0.1\lambda_x$ to $0.3\lambda_x$, i.e. for a range

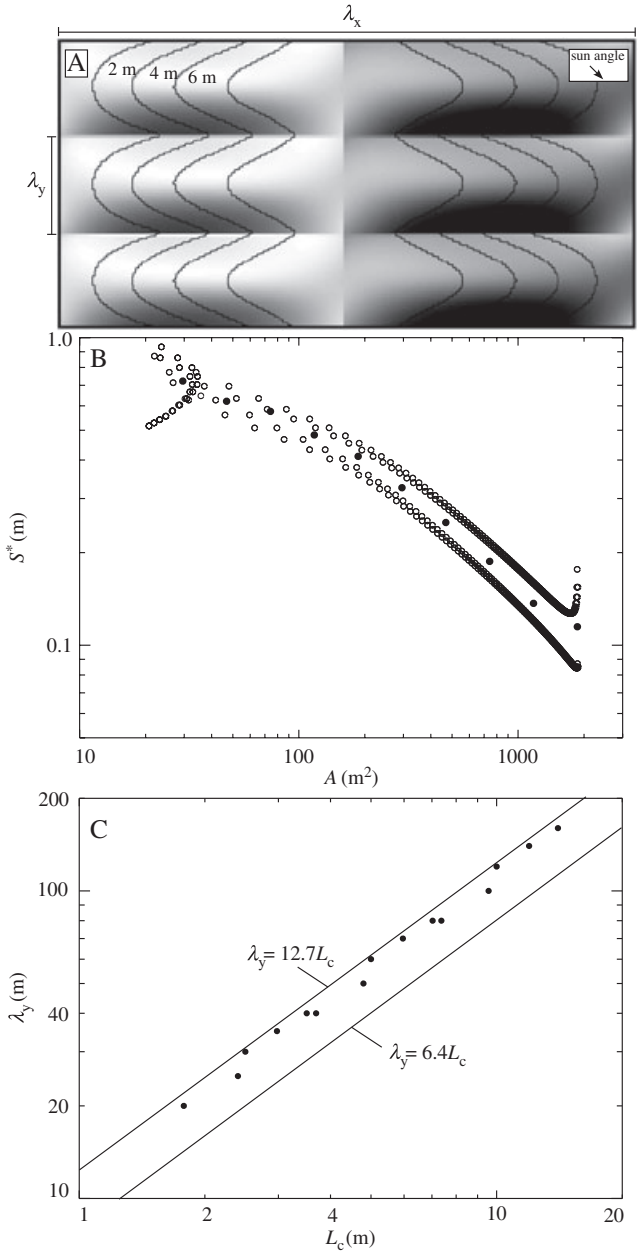

Figure 7. Results of the λ_y versus L_c method of Perron *et al.* (2009) on the synthetic landscape represented by Equation (13). (A) Shaded relief image of the synthetic landscape for a specific example with $\lambda_x = 200$ m and $\lambda_y = 25$ m. (B) Plot of the values of S^* and A for the example in (A). Open circles are all of the data points, closed circles are the logarithmically-binned averages. The values of D/K, m, and λ_y/L_c values in this example are 2.4 m, 0.47, and 10.4, respectively. This procedure was repeated for a total of 15 cases with a range of values of λ_x (from 200 to 800 m) and λ_y (from $0.1\lambda_x$ to $0.3\lambda_x$, i.e. for a ratio of spacing of second-order valleys to first-order valleys between 3 and 10). (C) A plot of the results illustrate that λ_y is proportional to L_c with a coefficient of between 6.4 and 12.7 for all cases.

of ratios of the spacing of second-order valleys to first-order valleys of between 3.3 and 10). The results (Figure 7(C)) illustrate that λ_y is proportional to L_c with a coefficient of between 6.4 and 12.7 in all cases. Values of m, obtained from least-squares fits to plots analogous to Figure 7(B), vary from 0.4 to 0.5. The value of L_c is proportional to λ_x by construction. As such, this analysis can be performed at any value of λ_x with identical results. Similarly, λ_y/L_c is independent of h_0 because L_c does not depend on h_0 for Equation (13), i.e. D/K is based on $|\nabla z|/(\nabla^2 z - \nabla^2 z_h)$, and the latter is independent of h_0. As such, the ratio λ_y/L_c depends only on the ratio λ_x/λ_y. The fact that Equation (13) yields the result $6.4 \leq \lambda/L_c \leq 12.7$ for a wide range of parameters further suggests that $6.4 \leq \lambda/L_c \leq 12.7$ is not diagnostic of DL conditions or any specific value of θ_c.

Mapping of the Relative Importance of DL Versus TL Conditions Using Soil Texture

Soil texture datasets provide preliminary constraints on the relative importance of DL versus TL conditions at a given study site. Figure 8(A) and 8(B) illustrate grayscale maps of the ratio of sand and rock fragments to silt and clay in the conterminous USA using the CONUS soil datasets of Miller and White (1998). Figure 8(B) illustrates the data in diagnostic ranges, with dark gray representing areas that are DL dominated (defined as having a ratio of sand and rock fragments to silt and clay less than 0.5), white areas representing areas that are TL dominated (defined as a ratio greater than 2) and medium gray areas representing areas that are a combination of TL and DL conditions in roughly equal proportion (defined as having a ratio between 0.5 and 2.0). According to these maps, TL conditions dominate in mountainous areas of the western USA and in areas where the parent material is sand dominated (e.g. Nebraska Sand Hills, Atlantic Coastal Plain). DL conditions are predominant in low-relief areas of the Mississippi Valley and in areas where the parent material weathers to fine-grained colluvium and saprolite. The ratio of sand and rock fragments to silt and clay correlates with slope at the 1 km scale. Figure 8(C) plots the geometric mean of the ratio of sand and rock fragments to silt and clay, denoted here as R, as a function of the slope S computed at the 1 km scale. Low-relief regions (i.e. slopes less than 10%) have, on average, approximately equal quantities of sand/rock fragments and silt/clay, suggesting that TL and DL conditions are both significant in those areas. Regions with slopes above 20% (i.e. mountainous regions of the western USA) have, on average, ratios greater than 2.0, suggesting TL-dominated conditions for most mountainous areas. It should be emphasized that the correlation between the ratio R and slope S describes average behavior; many locations deviate from the average trends illustrated in Figure 8(C). Figure 8(A), for example, illustrates that much of the low-relief Atlantic Coastal Plain has high values of R, due to the sandy nature of the alluvial and marine deposits in that region, which is opposite to the mean trend of low R values in low-relief topography. Nonetheless, the relationship between the ratio R and slope S in Figure 8(C) suggests that, in general, TL conditions become more dominant as relief increases.

Conclusions

This paper addresses the question: under what conditions is the fluvial and slope-wash erosion of soil predominantly detachment limited versus transport limited? First, it is argued that many landscapes have variable erodibility and hence the relative importance of DL versus TL conditions requires an assessment of the relative rates of bed load and suspended load sediment transport from areas with different erodibilities, because areas of relatively high erodibility contribute disproportionately to the total erosion rate in any area with variable erodibility. Second, the role of soil texture in controlling the relative rates of bed load versus suspended load transport is documented, using theoretical calculations and available data sets from the literature that have measured bed load and suspended load in small drainage basins. Third, how spatial and temporal variations in detachment/entrainment thresholds can reconcile differing values of n_d and

n_t between studies in relatively homogeneous versus relatively heterogeneous landscapes is detailed. Fourth, the lack of a clear topographic attribute or measure, aside from the presence of distributary channel networks and incised valley floor deposits in some TL landscapes, for distinguishing between TL and DL conditions is illustrated. Finally, existing soil datasets were used to map the relative importance of DL and TL conditions in the conterminous USA by adopting the preliminary conclusion that TL and DL conditions occur in approximate proportion to the ratio of sand and rock fragments to silt and clay in the eroding soil. As the literature review in this paper suggests, our understanding of the relative importance of DL and TL

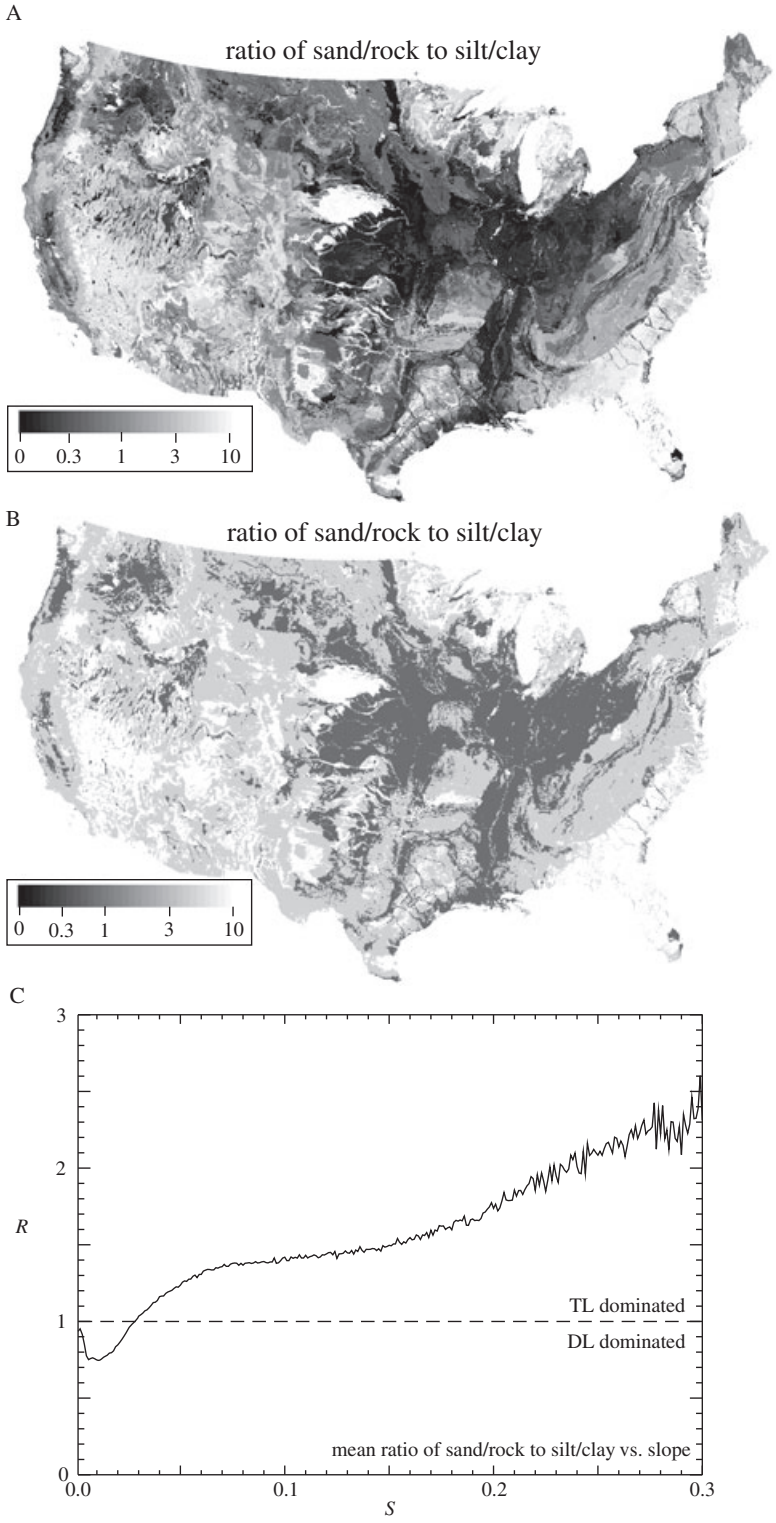

Figure 8. Map of the relative importance of DL versus TL conditions in the conterminous USA and relationships with topographic slope, based on the preliminary conclusion that relative importance of TL versus DL conditions is equal to the ratio of sand and rock fragments to silt and clay in the eroding soil. (A) and (B) Grayscale maps of the ratio of sand and rock fragments to silt and clay for the conterminous USA using the CONUS soil datasets of Miller and White (1998). (B) illustrates the data in diagnostic ranges, with dark gray representing areas that are DL dominated (defined as having a ratio of sand and rock fragments to silt and clay of less than 0.5), white areas representing areas that are TL dominated (defined as a ratio greater than 2) and medium gray areas representing areas that are both TL and DL in roughly equal proportion (defined as having a ratio between 0.5 and 2.0). (C) Plot of the geometric mean of the ratio of sand and rock fragments to silt and clay, denoted here as R, as a function of the slope S computed at the 1 km scale.

conditions in specific study sites would greatly benefit from additional long-term measurements of sediment transport rates at the spatial scale of hillslopes and low-order valleys.

Acknowledgements—This study was partially funded by the Army Research Office Project No. 55104-EV. I wish to thank two anonymous reviewers and the associate editor for their constructive comments.

References

Abrahams AD, Parsons AJ, Luk SH. 1989. Distributions of depth of overland flow on desert hillslopes and its implications for modeling soil erosion. *Journal of Hydrology* **106**: 177–184.

Abrahams AD, Parsons AJ, Luk SH. 1991. The effect of spatial variability in overland flow on the downslope pattern of soil loss on a semiarid hillslope, southern Arizona. *Catena* **18**: 255–270.

Benda L, Hassan MA, Church M, May CL. 2005. Geomorphology of steepland headwaters: the transition from hillslopes to channels. *Journal of the American Water Resources Association* **41**: 835–851.

Bullock MS, Nelson SD, Kemper WD. 1988. Soil cohesion as affected by freezing, water content, time, and tillage. *Soil Science Society of America Journal* **52**: 770–776.

Carson MA, Kirkby MJ. 1972. Hillslope Form and Process. Cambridge University Press.

Culling WEH. 1960. Analytical theory of erosion. *Journal of Geology* **68**: 336–344.

Culling WEH. 1963. Soil creep and the development of hillside slopes. *Journal of Geology* **71**: 127–161.

Davy P, Crave A. 2000. Upscaling local-scale transport processes in large-scale relief dynamics. *Physics and Chemistry of Earth, Part A Solid Earth Geodynamics* **25**: 533–541.

Davy P, Lague D. 2009. Fluvial erosion/transport equation of landscape evolution models revisited. *Journal of Geophysical Research* **114**, F03007, doi:10.1029/2008JF001146.

Duncan SH, Bilby RF, Ward JW, Heffner JT. 1987. Transport of road-surface sediment through ephemeral stream channels. *Water Resources Bulletin* **23**: 113–119.

Dyrness CT. 1969. Hydrologic properties of soils on three small watersheds in the Western Cascades of Oregon. USDA Forest Service Research Paper PNW-111. Pacific Northwest Forest & Range Experiment Station, Portland, Oregon.

Eckern PC. 1950. Raindrop impact as the force initiating soil erosion. *Proceedings of the Soil Science Society of America* **15**: 7–10.

Emmett WW, Wolman MG. 2001. Effective discharge and gravel-bed rivers. *Earth Surface Processes and Landforms* **26**: 1369–1380.

Ferguson RI, Church M. 2004. A simple universal equation for grain settling velocity. *Journal of Sedimentary Research* **74**: 933–937.

Fredriksen RL. 1970. Erosion and sedimentation following road construction and timber harvest on unstable soils in three small western Pacific Oregon watersheds. USDA Forest Service Research Paper PNW-104. Pacific Northwest Forest & Range Experiment Station, Portland, Oregon.

Gabet EJ, Dunne T. 2003. Sediment detachment by rain power. *Water Resources Research* **39** doi:10.1029/2001WR000656.

Goodrich DC, Lane LJ, Shillito RM, Miller SN, Syed KH, Woolhiser DA. 1997. Linearity of basin response as a function of scale in a semiarid watershed. *Water Resources Research* **33**: 2951–2965.

Hack JT. 1957. Studies of longitudinal stream profiles in Virginia and Maryland. US Geological Survey Professonal Paper 294-B; 45–97.

Hairsine P, Rose C. 1992. Modeling water erosion due to overland flow using physical principles 2: rill flow. *Water Resources Research* **28**: 245–250.

Howard AD. 1994a. Badlands. In Geomorphology of Desert Environments, Abrahams AD, Parsons AJ (eds). Chapman and Hall: London; 213–242.

Howard AD. 1994b. A detachment-limited model of drainage basin evolution. *Water Resources Research* **30**: 2261–2285.

Howard AD, Kerby G. 1983. Channel changes in badlands. *Geological Society of America Bulletin* **94**: 739–752.

Ijjasz-Vasquez EJ, Bras RL. 1995. Scaling regimes of local slope versus contributing area in digital elevation models. *Geomorphology* **12**: 299–311.

Istanbulluoglu E, Tarboton DG, Pack RT, Luce C. 2003. A sediment transport model for incision of gullies on steep topography. *Water Resources Research* **38**(4), doi:10.1029/2002WR001467.

Kemper WD, Rosenau RC. 1984. Soil cohesion as affected by time and water content. *Soil Science Society of America Journal* **48**: 1001–1006.

Lane LJ. 1982. Development of a procedure to estimate runoff and sediment transport in ephemeral streams. In Recent Developments in the Explanation and Prediction of Erosion and Sediment Yield. IAHS Publication No. 137; **275**–282.

Leopold LB, Maddock Jr T. 1953. The hydraulic geometry of stream channels and some physiographic implications. US Geological Survey Professional Paper 252.

McCool DK, Brown LC, Foster GR, Mutchler CK, Meyer LD. 1987. Revised slope steepness factor for the universal soil loss equation. *Trans. ASAE* **30**: 1387–1396.

Melton MA. 1957. An analysis of the relations among elements of climate, surface properties, and geomorphology. Department of Geology of Columbia University Technical Report 11, Project NR 389–042, Office of Naval Research, New York.

Miller DA, White RA. 1998. A Conterminous United States Multi-Layer Soil Characteristics Data Set for Regional Climate and Hydrology Modeling. Version 2. Penn State Soil Information for Environmental Modeling and Ecosystem Management. Digital Data available online at http://www.soilinfo.psu.edu/index.cgi?soil_data&conus

Milliman JD, Syvitski JPM. 1992. Geomorphic/tectonic control of sediment discharge to the ocean: the importance of small mountainous river. *Journal of Geology* **100**: 525–544.

Moglen GE, Bras RL. 1995a. The effect of spatial heterogeneities on geomorphic expression in a model of basin evolution. *Water Resources Research* **31**: 2613–2623.

Moglen GE, Bras RL. 1995b. The importance of spatially heterogeneous erosivity and the cumulative area distribution within a basin evolution model. *Geomorphology* **12**: 173–185.

Montgomery DR, Brandon MT. 2002. Topographic controls on erosion rates in tectonically active mountain ranges. *Earth and Planetary Science Letters* **201**: 481–489.

Nanson GC. 1974. Bedload and suspended-load transport in a small, steep, mountain stream. *American Journal of Science* **274**: 471–486.

Nearing MA, Kimoto A, Nichols MH, Ritchie JC. 2005. Spatial patterns of soil erosion and deposition in two small, semiarid watersheds. *Journal of Geophysical Research* **110**: F04020. doi:10.1029/2005JF000290.

Nearing MA, Simanton JR, Norton LD, Bulygin SJ, Stone J. 1999. Soil erosion by surface water flow on a stony, semiarid hillslope. *Earth Surface Processes and Landforms* **24**: 677–686.

Osterkamp WR. 2008. Geology, soils, and geomorphology of the Walnut Gulch Experimental Watershed, Tombstone, Arizona. *Journal of the Arizona-Nevada Academy of Sciences* **40**: 136–154.

Parsons AJ, Brazier RE, Wainwright J, Powell DM. 2006. Scale relationships in hillslope runoff and erosion. *Earth Surface Processes and Landforms* **31**: 1384–1393.

Pelletier JD. 2010. Minimizing the grid-resolution dependence of flow-routing algorithms for geomorphic applications. *Geomorphology* **122**: 91–98.

Perron JT, Dietrich WE, Kirchner JW. 2008. Controls on the spacing of first-order valleys. *Journal of Geophysical Research* **113**: F04016, doi:10.1029/2007JF000977.

Perron JT, Kirchner JW, Dietrich WE. 2009. Formation of evenly-spaced ridges and valleys. *Nature* **460**: 502–505.

Prosser IP, Dietrich WE. 1995. Experiments on erosion by overland flow and their implication for a digital terrain model of channel initiation. *Water Resources Research* **31**: 2867–2876.

Ritchie JC, Nearing MA, Nichols MH, Ritchie CA. 2005. Patterns of soil erosion and redeposition on Lucky Hills watershed, Walnut Gulch Experimental watershed, Arizona. *Catena* **61**: 122–130.

Ritchie JC, Nearing MA, Rhoton FE. 2009. Sediment budgets and source determination using fallout Cesium-137 in a semiarid rangeland watershed, Arizona, USA. *Journal of Environmental Radioactivity* **100**: 637–643.

Rose CW. 1960. Soil detachment caused by rainfall. *Soil Science* **89**: 28–35.

Schoorl JM, Sonneveld MPW, Veldkamp A. 2000. Three-dimensional landscape process modelling: the effect of DEM resolution. *Earth Surface Processes and Landforms* **25**: 1025–1034.

Schumm SA. 1956. The role of creep and rainwash on the retreat of badland slopes [South Dakota]. *American Journal of Science* **254**: 693–706.

Seidl MA, Dietrich WE, Kirchner JW. 1994. Longitudinal profile development into bedrock: an analysis of Hawaiian channels. *Journal of Geology* **102**: 457–474.

Simanton JR, Renard KG. 1982. Seasonal change in infiltration and erosion from USLE plots in southeastern Arizona. *Hydrology and Water Resources in Arizona and the Southwest* **12**: 37–46.

Simanton JR, Osterkamp WR, Renard KG. 1993. Sediment yield in a semiarid basin: sampling equipment impacts. In Sediment Problems; Strategies for Monitoring, Prediction and Control, Proceedings of the Yokohama Symposium, July 1993. IAHS Publication No. 217: 3–9.

Simpson G, Schlunegger F. 2003. Topographic evolution and morphology of surfaces evolving in response to coupled fluvial and hillslope sediment transport. *Journal of Geophysical Research* **108**: 2300, doi:10.1029/2002JB002162.

Smith TR, Bretherton FP. 1972. Stability and the conservation of mass in drainage basin evolution. *Water Resources Research* **8**: 1506–1529.

Tarboton DG. 1997. A new method for the determination of flow directions and upslope areas in grid Digital Elevation Models. *Water Resources Research* **33**: 309–319.

Tarboton DG, Bras RL, Rodriguez-Iturbe I. 1992. A physical basis for drainage density. *Geomorphology* **5**: 59–76.

Tucker GE, Bras RL. 1998. Hillslope processes, drainage density, and landscape morphology. *Water Resources Research* **34**: 2751–2764.

Turowski JM, Rickenmann D, Dadson SJ. 2010. The partitioning of the total sediment load of a river into suspended load and bedload: a review of empirical data. *Sedimentology* **57**: 1126–1146.

Van De Wiel MJ, Coulthard TJ, Macklin MG, Lewin J. 2007. Embedding reach-scale fluvial dynamics within the CAESAR cellular automaton landscape evolution model. *Geomorphology* **90**: 283–301.

Weissmann GS, Hartley AJ, Nichols GJ, Scuderi LA, Olson M, Buehler H, Banteah R. 2010. Fluvial form in modern continental sedimentary basins: distributive fluvial systems. *Geology* **38**: 392.

Whipple KX, Tucker GE. 1999. Dynamics of the stream-power river incision model: implications for the height limits of mountain ranges, landscape response timescales, and research needs. *Journal of Geophysical Research* **104**: 17661–17674.

Whipple KX, Tucker GE. 2002. Implications of sediment-flux-dependent river incision models for landscape evolution. *Journal of Geophysical Research* **107**: doi:10.1029/2000JB000044.

Willgoose G. 2005. Mathematical modeling of whole landscape evolution. *Annual Reviews of Earth and Planetary Sciences* **33**: 443–459.

Willgoose G, Bras RL, Rodriguez-Iturbe I. 1991. A coupled channel network growth and hillslope evolution model 1. Theory. *Water Resources Research* **27**: 1671–1684.